J Appl Electrochem (2013) 43:855–863
DOI 10.1007/s10800-013-0569-7

ORIGINAL PAPER

# Voltammetric determination of alkannin using an Au nanoparticles–poly(diallyldimethylammonium chloride)-functionalized graphene nanocomposite film

**Letao Wang · Daban Lu · Shasha Yu · Xuezhao Shi · Chunming Wang · Yan Zhang**

Received: 2 April 2013 / Accepted: 23 May 2013 / Published online: 5 June 2013


**Abstract** An electrochemical sensor based on Au nanoparticles (AuNPs)–poly(diallyldimethylammonium chloride) (PDDA)-functionalized graphene (AuNPs–PDDA-G) nanocomposite was fabricated for the sensitive detection of alkannin. The nanocomposite was characterized by X-ray diffraction, ultraviolet/visible spectra, scanning electron microscopy, and transmission electron microscopy. Cyclic voltammetry and differential pulse voltammetry were used to investigate the electrochemical behaviors of alkannin on the AuNPs–PDDA-G nanocomposite film-modified glassy carbon electrode. This electrochemical sensor displayed satisfactory analytical performance for alkannin detection over a range from 5.0 nmol $L^{-1}$ to 3.0 μmol $L^{-1}$ with a detection limit of 1.4 nmol $L^{-1}$ ($S/N = 3$). Moreover, the sensor also exhibited good reproducibility and stability, and could be used for the detection of alkannin in real samples with satisfactory results.

**Keywords** AuNPs · PDDA · Graphene · Alkannin · Electrochemical determination

## 1 Introduction

Isohexenylnaphthazarins, as lipophilic hydroxynaphthoquinone (HNQ) red pigment, are used as additives to food and cosmetics. Alkannins (Fig. 1) as a isohexenylnaphthazarins derivater can be found in the outer surface of the roots of at least 150 species that belong to the genera Alkanna, Lithospermum, Echium, Onosma, Anchusa, and Cynoglossum of the Boraginaceae family [1]. The alkannin is potent pharmaceutical substances with a well established and wide spectrum of wound healing, antimicrobial, anti-inflammatory, antioxidant, anticancer, and antithrombotic biological activity, as have been described extensively in review papers of the Papageorgiou group [2, 3]. In addition, as a lipophilic red pigment, the alkannin has a wide application in cosmetic formulations, food colorants, and additives [4]. Therefore, it is necessary to establish some rapid, simple, and accurate approaches for the determination of alkannin. Some analytical methods, such as ultraviolet (UV) spectrometry [5], high performance liquid chromatography (HPLC) [6, 7], and capillary electrophoresis [8, 9], have been used in the determination of alkannin. However, these techniques are time-consuming and expensive. In addition, these techniques also require skilled operators and complicated instrumentations. It is well known that electrochemical method has the advantages of fast response speed, cheap instrument, inexpensiveness, simple operation, timesaving, high sensitivity, excellent selectivity, and real-time detection in situ condition as an analytical technique [10]. Chaisuksant et al. [11] determined the alkannin by electrochemical method using glassy carbon electrode (GCE). There is also, to the best of our knowledge, no report based on using modified electrodes for the determination of alkannin.

Graphene, a two-dimensional carbon material, has attracted much more attention for both fundamental research and technological applications. Graphene has a lot of advantages, such as high conductivity, superior mechanical, and electronic properties, producing promising potential applications in sensors and electrocatalysis [12–15]. However, graphene is hydrophobic and tends to form

L. Wang · D. Lu · S. Yu · X. Shi · C. Wang (✉) · Y. Zhang (✉)
College of Chemistry and Chemical Engineering, Lanzhou University, Lanzhou 730000, People's Republic of China
e-mail: wangcm@lzu.edu.cn

Y. Zhang
e-mail: zhangy01@lzu.edu.cn

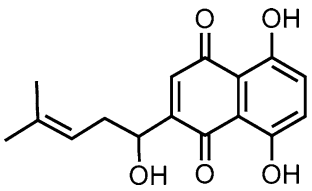


**Fig. 1** Chemical structure of alkannin

agglomerates which may limit its further applications [16]. Particularly in electrochemical sensors, the prevention of aggregation is of vital importance for graphene because most of its unique properties are only associated with individual sheets [17]. As a linear positively charged polyelectrolyte, poly(diallyldimethylammonium chloride) (PDDA) has been found to be an effective material to noncovalently functionalize graphene sheets [18]. The PDDA-G has more functional groups than graphene. The more functional groups are beneficial for the absorption of the analyte by electrostatic interaction. Moreover, the positive PDDA-functionalized graphene (PDDA-G) reported in our previous work [17] exhibited good conductivity, solubility, and biocompatibility. On the other hand, gold nanoparticles (AuNPs) are one of most stable metal nanoparticles. Due to its novel optical, electrical, catalytic properties, and favorable biocompatibility, AuNPs have been widely applied in analytical chemistry [19]. In our previous work, AuNPs can be used to construct the biosensor for electrochemical determination of $H_2O_2$ [20]. Combining the properties of functionalized graphene, such as high specific surface area, excellent conductivity, and solubility, with the catalytic properties of AuNPs, the AuNPs–PDDA-G nanocomposite should be beneficial to develop highly sensitive sensors.

Herein, a novel alkannin electrochemical sensor based on AuNPs–PDDA-G nanocomposite was introduced. The fabricated electrochemical sensor employed for the voltammetric determination of alkannin in the acetic acid–sodium acetate (HAc–NaAc) buffer solution (pH 5.0), and showed excellent electrocatalytic activity toward alkannin with a wide linear range and low detection limit. Moreover, in practical application investigations, the fabricated electrode showed good recoveries and could be applied to determine alkannin in pharmaceuticals. Therefore, this study offers a new way to broaden the analytical applications of functionalized graphene with metal NPs in pharmaceutical analysis.

## 2 Experimental

### 2.1 Reagents and apparatus

Graphite powder (KS-10) and alkannin were from Alfa Aesar (Beijing, China). PDDA (20 %) was purchased from Sigma. Hydrazine hydrate and chloroauric acid were from Nanjing Reagent Co., Ltd. The Lithospermum was purchased from local drugstore. All other reagents and solvents were of analytical grade and used without further purification. All chemicals were prepared with deionized water purified via Milli-Q unit.

Electrochemical measurements were performed on a CHI 1210A electrochemical workstation (ChenHua Instrument, China) with a three-electrode system consisting of a platinum wire auxiliary, a saturated calomel reference, and a bare or modified GCE working electrode. UV–Vis spectra were obtained on a UV-3600 (Shimadzu) UV–Vis spectrophotometer. The morphology of the samples was observed using field-emission scanning electron microscopy (FESEM, S-4800, Hitachi, Japan) and transmission electron microscopy (TEM, Tecnai G2 F30, FEI, USA). X-ray diffraction (XRD) data were collected on XRD-6000 (Shimadzu, Tokyo, Japan) using Cu Kα (1.5406 Å) radiation.

### 2.2 Synthesis of AuNPs–PDDA-G nanocomposite

Graphite oxide (GO) was prepared from graphite powder by a modified Hummers and Offeman [21] method. 50 mg GO was dispersed in 100 mL deionized water to yield a yellow–brown dispersion by ultrasonication for 2 h. Subsequently, the homogeneous GO dispersion was mixed with 2.5 mL PDDA solution (20 %) and stirred for 30 min. Then, the PDDA-wrapped GO solution was mixed with $HAuCl_4$ and stirred for 1 h. The resulting mixture was further treated with 2.5 mL hydrazine hydrate and allowed to react for 24 h at 90 °C. Finally, the obtained AuNPs–PDDA-G nanocomposite was separated by centrifugation and further washed with water. The PDDA-functionalized graphene was prepared by the same procedure without the $HAuCl_4$.

### 2.3 Fabrication of electrochemical sensor

Prior to the surface modification, the bare GCE was polished to obtain a mirror-like surface with 0.3 and 0.05 μm γ-alumina, then washed successively with anhydrous alcohol and doubly distilled water in an ultrasonic bath, and dried in room temperature. The AuNPs–PDDA-G nanocomposite was dissolved in deionized water at a concentration of 0.5 mg $mL^{-1}$ with the aid of ultrasonic agitation for 6 h, resulting in a homogeneous black suspension. Afterword, 5 μL AuNPs–PDDA-G nanocomposite solution was deposited on the fresh prepared GCE surface. The electrode was dried in the room temperature. The obtained electrode was noted as AuNPs–PDDA-G/GCE.

### 2.4 Preparation of real samples

Lithospermum was finely crushed in a mortar. Then, 500 mg of the Lithospermum powder was accurately weighed and dispersed in 25 mL of ethanol with reflux for 1 h. After filtration, the filter cake was refluxed for 1 h twice using 25 mL of ethanol each time, and all filtrates were transferred into a 250 mL calibrated flask and diluted to volume with ethanol.

### 2.5 Electrochemical measurements

Before electrochemical experiments, the solution was bubbled with nitrogen for 30 min to remove dissolved oxygen, and all the experiments were carried out at room temperature. About 10 mL of the HAc–NaAc buffer solution (pH 5.0) containing an appropriate amount of alkannin standard solution or sample was added into the electrochemical cell and then the three-electrode system was installed on it. The CVs were recorded in the potential range from −0.40 to 0.00 V with a scan rate of 50 mV $s^{-1}$. DPV was carried out with the parameters of increment potential, 0.004 V; pulse amplitude, 0.05 V; pulse width, 0.05 s; sample width, 0.0167 s; pulse period, 0.2 s; quiet time, 2 s.

### 2.6 Chromatographic analysis

Samples were also validated and analyzed by HPLC. The HPLC system consisted of a binary pump, a degasser, an automated injector, a column oven, and an UV–Vis detector (all Agilent 1100 Series, USA). HPLC was also introduced to detect alkannin in drug according to Papageorgiou and co-workers [1] with a slight modification. The column was a $C_{18}$ analytical column (4.6 mm × 250 mm × 5 μm). The mobile phase (acetonitrile/deionized 85:15) is pumped at a flow rate of 0.8 mL $min^{-1}$. The detection was performed at a wavelength of 516 nm for alkannin with UV–Vis spectra detector. The column temperature was room temperature.

## 3 Results and discussion

The AuNPs–PDDA-G/GCE was prepared by a simple procedure. The main steps are summarized in Scheme 1. First was the functionalization of GO by PDDA. The PDDA adsorb on the GO by the noncovalent adsorption. Then, the $N_2H_2{\cdot}H_2O$ was selected as the reductant and the PDDA-GO and $HAuCl_4$ were reduced to AuNPs–PDDA-G. After that, the AuNPs–PDDA-G aqueous solution was dropped on the cleaned GCE and dried in the air. Combining the properties of functionalized graphene, such as high specific surface area and excellent conductivity, with the AuNPs, the AuNPs–PDDA-G/GCE exhibited an excellent electrochemical activity of alkannin.

### 3.1 Characterizations of AuNPs–PDDA-G nanocomposite

The morphology of AuNPs–PDDA-G nanocomposite was characterized using SEM and TEM. As can be seen in Fig. 2A, it clearly shows the thin flake-like shapes with some corrugation suggesting a flexible structure of the nanosheets and almost all anchored AuNPs were distributed homogeneously on the sheet surface with negligible

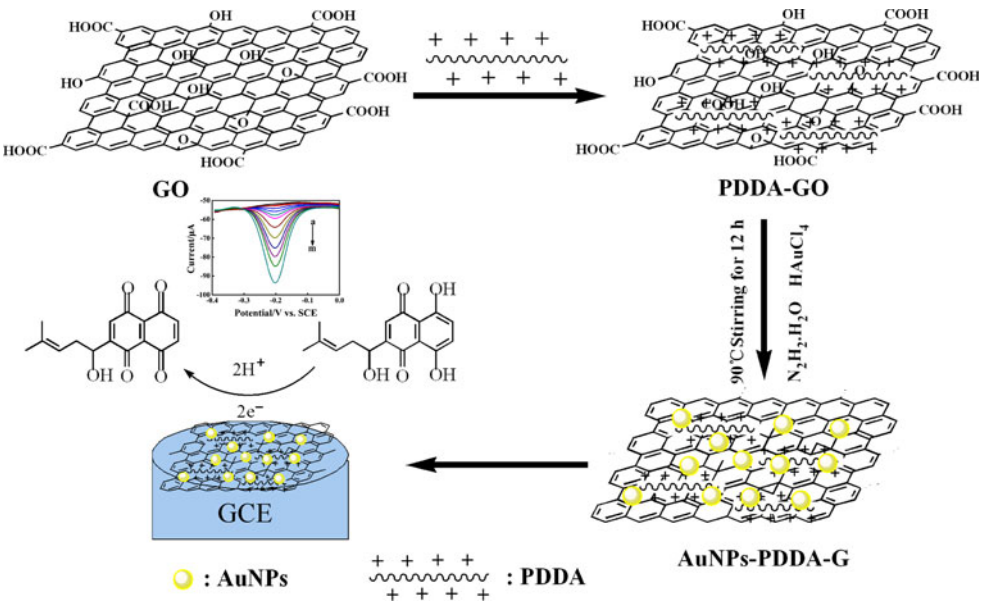


**Scheme 1** The proposed schemes of the AuNPs–PDDA-G/GCE and alkannin determination

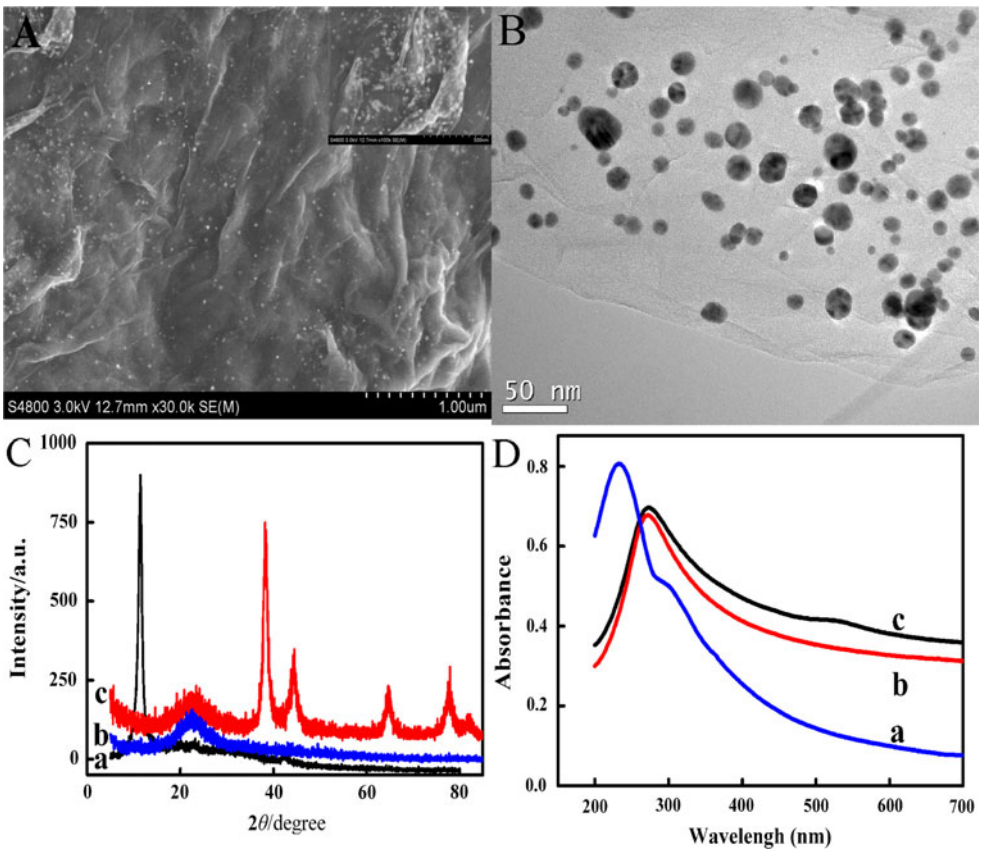


**Fig. 2** SEM (**A**) and TEM (**B**) of AuNPs–PDDA-G; XRD spectrums (**C**): (*a*) GO, (*b*) PDDA-G, (*c*) AuNPs–PDDA-G; UV–Vis spectrums (**D**): (*a*) GO, (*b*) PDDA-G, (*c*) AuNPs–PDDA-G

nanoparticle agglomeration. The TEM image (Fig. 2B) shows that AuNPs with an average diameter of about 25 nm are uniformly distributed on the wrinkled surface of the PDDA-G. Furthermore, highly dispersed AuNPs on supports with larger surface areas have advantages in sensor sensitivity.

The functionalized graphene was characterized by XRD. As comparison, the PDDA-GO is reduced by the $N_2H_4{\cdot}H_2O$, and the XRD pattern is exhibited in Fig. 2C. Figure 2C shows the XRD pattern of GO (Fig. 2C curve a) had a characteristic peak centered about at 11.0°, but the PDDA-G (Fig. 2C curve b) appeared a peak centered at 22.5°, in agreement with previous report [17], indicating that GO was reduced to graphene by hydrazine hydrate. Moreover, compared with the spectra of PDDA-G, the AuNPs–PDDA-G (Fig. 2C curve c) besides the peak originating from the PDDA-G, the diffraction peaks at 38.6°, 44.8°, 64.9°, and 77.9° can be well indexed to the (111), (200), (220), and (311) planes of AuNPs [22]. The UV–Vis absorption spectrum was also used to confirm the formation of the composite as shown in Fig. 2D. All of the samples were prepared in aqueous medium to collect their UV–Vis spectra. As could be seen, the GO (Fig. 2D curve a) shows a strong absorption peak at 231 nm and a shoulder peak at 300 nm, which corresponded to $\pi \rightarrow \pi^*$ transitions of aromatic C=C bond and $n \rightarrow \pi^*$ transition of C=O bond, respectively [23]. PDDA-G (Fig. 2D curve b) shows a strong absorption peak at 270 nm which referred to $\pi \rightarrow \pi^*$ transitions of aromatic C=C bond indicating the restoration of the $\pi$-conjugation network of the graphene nanosheets. Meanwhile, the band of $n \rightarrow \pi^*$ transition of C=O at about 300 nm was disappeared hinting the complete reduction of GO [24]. After the AuNPs were deposited, the characteristic peak of AuNPs was observed in

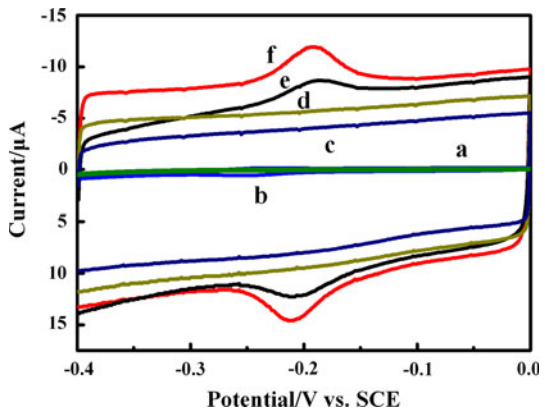


**Fig. 3** Cyclic voltammograms recorded of absence (*a*, *c*, *d*) and presence (*b*, *e*, *f*) 1.0 μmol $L^{-1}$ alkannin at bare GCE (*a*, *b*), PDDA-G/GCE (*c*, *e*), AuNPs–PDDA-G/GCE (*d*, *f*) in 0.2 mol $L^{-1}$ HAc–NaAc buffer solution (pH 5.0) with a scan rate of 50 mV $s^{-1}$

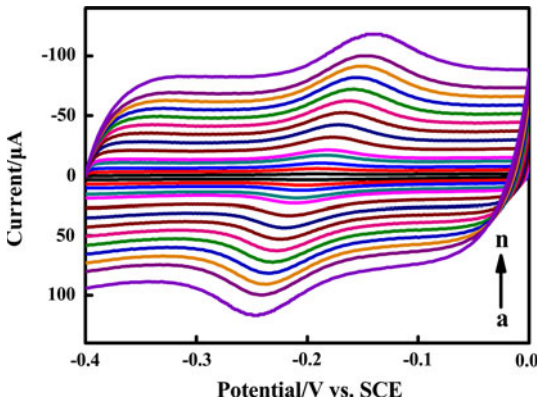


**Fig. 4** Cyclic voltammograms of AuNPs–PDDA-G/GCE in 0.2 mol $L^{-1}$ HAc–NaAc buffer solution containing 1.0 μmol $L^{-1}$ alkannin at various scan rates: (*a–n*) 30, 50, 80, 100, 120,150, 200, 250, 300, 350, 400, 450, 500, and 600 mV $s^{-1}$

AuNPs–PDDA-G (Fig. 2D curve c) at 526 nm which indicated the efficient adsorption of AuNPs onto the nanosheets surface.

### 3.2 Electrochemical behavior of alkannin

The electrochemical behaviors of 1.0 μmol $L^{-1}$ alkannin on different electrodes were studied by CV in 0.2 mol $L^{-1}$ HAc–NaAc buffer solution (pH 5.0) at a scan rate of 50 mV $s^{-1}$. At the bare GCE (Fig. 3 curve b), alkannin shows rather poor redox current peaks at $E_{pa} = -0.250$ V and $E_{pc} = -0.117$ V. On the PDDA-G/GCE (Fig. 3 curve e), the redox peak currents are significantly increased, which are about 10 times higher than those at the bare GCE, which might be attributed to the excellent conductivity and large surface area of graphene. However, in the case of AuNPs–PDDA-G/GCE (Fig. 3 curve f), a pair of well-defined and quasi-reversible redox peaks of alkannin is obtained at $E_{pa} = -0.211$ V and $E_{pc} = -0.186$ V with peak-to-peak separation ($\Delta E_p$) of about 25 mV, revealing a fast electron-transfer process. The AuNPs–PDDA-G/GCE shows the largest redox peak currents compared to PDDA-G/GCE and bare electrode. The remarkably enhanced voltammetric response of alkannin could be reasonably ascribed to the doping of AuNPs, which improves the absorption efficiency and electrochemical reactivity of alkannin. The above results suggest that AuNPs effectively modified the surface of the graphene sheets, which provide an efficient interface and microenvironment for the electrochemical reaction of alkannin. The combination of functionalized graphene and AuNPs improves the electronic transport capacity of the electrode and accelerate the electron-transfer rate.

Moreover, no redox peaks are observed at Au–PDDA-G/GCE in blank buffer solution (Fig. 3 curve d), indicating that the Au–PDDA-G/GCE is non-electroactive in the selected potential region. The back ground current of the

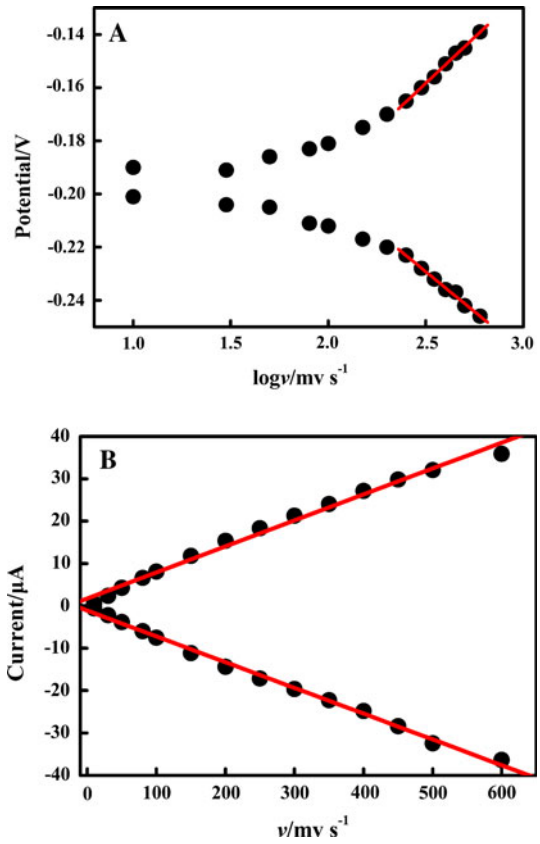


**Fig. 5** **a** The relationship between the peak current and scan rate. **b** The relationship between the peak potential and scan rate. On the AuNPs–PDDA-G/GCE, 0.2 mol $L^{-1}$ HAc–NaAc buffer solution containing 1.0 μmol $L^{-1}$ alkannin

Au–PDDA-G/GCE was lager than the PDDA-G/GCE when no alkannin was added, which might attribute to the larger specific surface area and high conductivity of the Au–PDDA-G.

To investigate the reaction kinetics, the influence of scan rate on the peak current of alkannin was also investigated. As can be seen in Fig. 4, the oxidation ($I_{pa}$) and reduction ($I_{pc}$) peak currents for alkannin increase regularly with increase of scan rates from 30 to 600 mV $s^{-1}$. The alkannin shows a pair of symmetrical redox peaks, the redox peak currents follow the linear regression equation of $I_{pa}$ (μA) = 1.76 + 0.0613 $v$ (mV $s^{-1}$) and $I_{pc}$ (μA) = −1.14 − 0.0608 $v$ (mV $s^{-1}$) with the $R = 0.995$ and 0.998, respectively (Fig. 5B). As we know, linear relationship between scan rate and peak currents is the character of an adsorption and desorption process. Therefore, the redox process of alkannin on the AuNPs–PDDA-G/GCE is an adsorption and desorption process.

Furthermore, the influence of scan rate on the redox peak potential was also investigated for calculated the kinetic parameters. With the increase of scan rate, the oxidation peak potential shifted positively and the

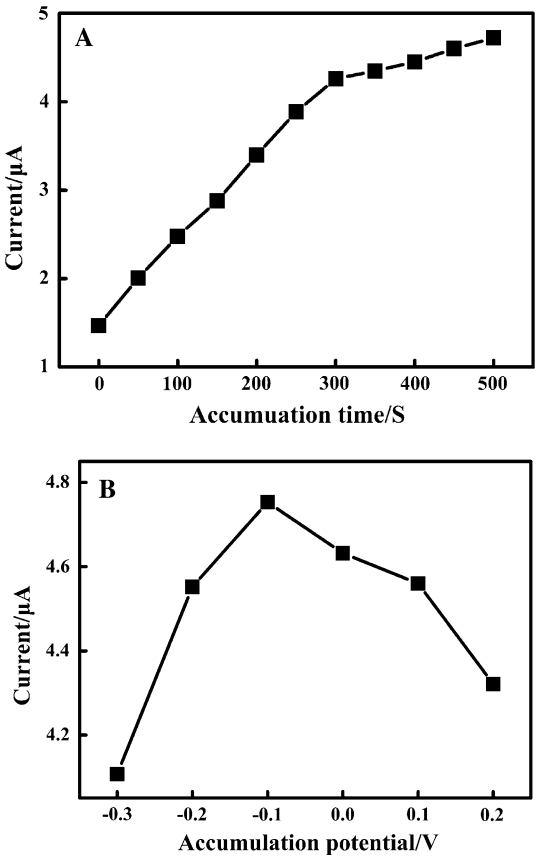


**Fig. 6** Effect of **a** accumulation time and **b** potential on the oxidation peak current of 1.0 μmol $L^{-1}$ alkannin in 0.2 mol $L^{-1}$ HAc–NaAc buffer solution (pH 5.0)

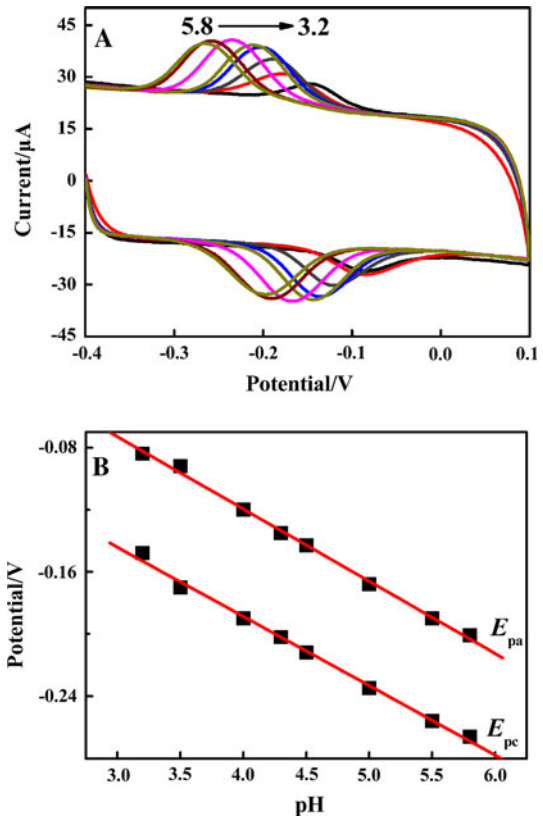


**Fig. 7** **a** Cyclic voltammograms of 1.0 μmol $L^{-1}$ alkannin at AuNPs–PDDA-G/GCE under different pHs. pH 5.8, 5.5, 5.0, 4.5, 4.2, 4.0, 3.5, and 3.2. **b** Effect of pH on the oxidation potential

reduction peak potential shifted negatively, and at higher scan rates, the anodic ($E_{pa}$) and cathodic ($E_{pc}$) peak potential showed linear relationship with the logarithm of scan rate (log $v$) (Fig. 5A). The linear relationship equation is $E_{pa}$ (V) $= -0.33 + 0.069 \log v$ (V $s^{-1}$, $R = 0.998$); $E_{pc}$ (V) $= -0.0788 - 0.06 \log v$ (V $s^{-1}$, $R = 0.996$). According to Laviron's model [25], the slope of the line for $E_{pa}$ and $E_{pc}$ could be expressed as $2.3RT/n(1-\alpha)F$ and $-2.3RT/n(1-\alpha)F$, respectively. Therefore, for alkannin, the electron-transfer coefficient ($\alpha$) and electron-transfer number ($n$) were calculated as 0.465 and 2.12. Additionally, the apparent heterogeneous electron-transfer rate constant ($k_s$) can also be obtained according to Ref. [25] based on the Eq. (1):

$$\log k_s = \alpha \log(1-\alpha) + (1-\alpha)\log\alpha - \log\frac{RT}{nFv} - \frac{\alpha(1-\alpha)nF\Delta E_p}{2.303RT}. \quad (1)$$

Here $n$ is the number of electrons involved in the reaction, $\Delta E_p$ is the peak-to-peak potential separation, $\alpha$ is the charge transfer coefficient, and $v$ is the scan rate. According to this equation, the $k_s$ for alkannin was calculated as 1.31 $s^{-1}$. According to the equation $Q_{ads} = nFA\Gamma$, the surface coverage ($\Gamma$) form the charge can be obtained as $1.55 \times 10^{-10}$ mol $cm^{-2}$ for Au–PDDA-G/GCE. The $\Gamma$ of PDDA-G and bare GCE was $9.05 \times 10^{-11}$ and $4.74 \times 10^{-12}$ mol $cm^{-2}$, respectively. The surface coverage of Au–PDDA-G/GCE was increased obviously, which would increase the adsorption capacity of alkannin, leading to enhance current response and decrease detection limit. The results could be attributed to the combination of AuNPs and PDDA-G, in which the AuNPs could increase the electrochemically adsorptive sites and the PDDA-G could also provide the large specific surface area to increase the adsorption of alkannin.

### 3.3 The optimal experimental conditions

It was believed that accumulation can improve the amount of alkannin absorbed on the electrode surface, and then improve determination sensitivity and decrease detection limit. Therefore, the effect of accumulation was investigated. The oxidation peak current of 1.0 μmol $L^{-1}$ alkannin at different accumulation time was compared. As shown in Fig. 6A, the oxidation peak current increased gradually with accumulation time up to 300 s. Afterward,

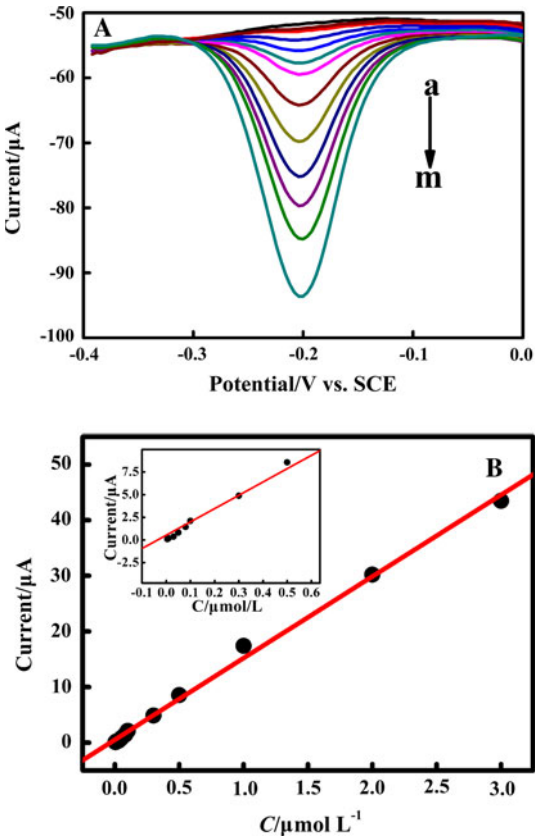


**Fig. 8** **A** DPV curves of AuNPs–PDDA-G/GCE in alkannin solution at different concentrations (*a*–*m*): 0, 0.005, 0.01, 0.03, 0.05, 0.08, 0.1, 0.3, 0.5, 0.8, 1.0, 2.0, and 3.0 μmol $L^{-1}$. **B** Plot of the peak current against the concentration of alkannin at AuNPs–PDDA-G/GCE

the peak current increased much slightly as further increasing accumulation time, suggesting that the accumulation of alkannin at AuNPs–PDDA-G/GCE rapidly reached saturation. Moreover, the influence of the accumulation potential on the oxidation peak current of alkannin was also tested. The highest oxidation peak current was achieved at −0.10 V (Fig. 6B). Thus, the accumulation step in the experiments was performed at −0.10 V for 300 s.

The influence of pH on the electrochemical behavior of alkannin was carefully studied. The maximum anodic peak current appeared at pH 5.0 (Fig. 7A) for the alkannin. With the further increase of buffer solution pH, the oxidation peak current decreased obviously. This could be related to the fact that proton took part in the electrochemical reaction. When the pH value was high, the shortage of proton prevented the oxidation and reduction of alkannin, leading to the decrease of current peak intensity. On the other hand, the diphenol, as it is well known, tends to form anions and makes the peak current decrease [26]. Therefore, pH 5.0 was selected as the optimum pH for the electrochemical detection of alkannin. In addition, in the selected pH range the formal peak potentials also negatively shift with the increase of solution pH, indicating that the proton is involved in the redox reaction of alkannin. As shown in Fig. 8B, the redox potential changes linearly with pH value, and the linear regression equations are $E_{pa}$ (V) = 0.560 − 0.054 pH ($R = 0.998$) and $E_{pc}$ (V) = 0.533 − 0.056 pH ($R = 0.999$). The slopes of the four regression equations were close to the theory value of 58.5 mV $pH^{-1}$. According to the following formula [25]: $dE_p/dpH = 2.303mRT/nF$, in which, $m$ is the number of proton, and $n$ is the number of electron, $m/n$ is calculated to be 0.95 for the oxidation and reduction process of alkannin. It indicates that the number of proton and electron involved in the electrochemical redox process of alkannin is equal. Therefore, the electrochemical redox of alkannin on the AuNPs–PDDA-G/GCE is a two-electron and two-proton process, and the electrode reaction equation is expressed as follow.

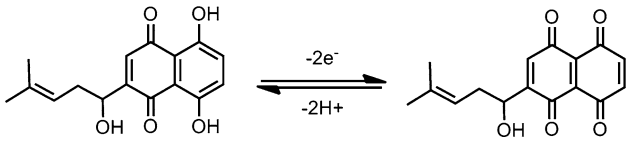


## 3.4 Determination of alkannin

As a highly sensitive and a low detection limit electrochemical method, differential pulse voltammetric (DPV) was used for the determination of alkannin at the proposed electrochemical sensor under the optimized conditions. Figure 8A shows the DPV curves of alkannin at the AuNPs–PDDA-G/GCE at various concentrations. The oxidation peak currents are proportional to the concentration of alkannin in a wider range of 5.0 nmol $L^{-1}$ to 3.0 μmol $L^{-1}$. The linear equation is $I$ (μA) = 14.67$C$ (μmol $L^{-1}$) + 0.528 ($R = 0.998$) (Fig. 8B), and the detection limit is as low as 1.4 nmol $L^{-1}$ ($S/N = 3$). The linear range and detection limit are better than those of previously reported sensors, such as PDDA-G (linear range: 94.72–378.9 nmol $L^{-1}$ and detection limit: 31.5 nmol $L^{-1}$) [27], bare GCE (detection limit: 0.55 mg $L^{-1}$) [11]. This lower detection limit could be attributed to the combination of AuNPs and PDDA-G, in which the AuNPs can increase the electrochemically adsorptive site and the PDDA-G could also provide the large specific surface area to increase the

**Table 1** The HPLC data of alkannin

| | Retention time (min) | Slope (a.u./mol $L^{-1}$)[a] | Intercept | $R^2$ |
|---|---|---|---|---|
| Alkannin | 5.6 | 2,928,940 | 89,632 | 0.9996 |

[a] In the linear range (1–250 μmol $L^{-1}$)

**Table 2** Determination of alkannin in medicine samples

| Sample | By HPLC (μmol $L^{-1}$)[a] | By this sensor (μmol $L^{-1}$)[b] | Add (μmol $L^{-1}$) | Found (μmol $L^{-1}$)[a] | RSD (%) | Rec. (%) |
|---|---|---|---|---|---|---|
| Alkanet extract 1 | 0.102 | 0.096<br>$F = 0.45$, $t = 0.13$ | 0.10 | 0.209 | 3.74 | 106.3 |
| Alkanet extract 2 | 0.682 | 0.677<br>$F = 0.51$, $t = 0.23$ | 0.30 | 0.963 | 2.76 | 98.5 |
| Tap water | 0 | 0<br>$F = -$, $t = -$ | 0.50 | 0.503 | 3.01 | 100.6 |

[a] Mean of three measurements

[b] The $F$ and $t$ values refer to comparison of the proposed method with HPLC. Theoretical values at 95 % confidence limits: $F = 19.00$, $t = 4.30$, - = mean of unvalued

adsorption of alkannin. Meanwhile, the electron-transfer on the electrode surface could be accelerated and the electrochemical signal is amplified due to the outstanding electric conductivity of PDDA-G. Therefore, sensitive detection of alkannin was achieved.

In order to prove the precision and practicability of the proposed method, the reproducibility of the AuNPs–PDDA-G/GCE was investigated. The fabrication reproducibility for ten AuNPs–PDDA-G/GCE was carried out by comparing the oxidation peak current of 1.0 μmol $L^{-1}$ alkannin. The relative standard deviation was 3.6 %, revealing that this method had good reproducibility. The selectivity of the sensor was also studied through the interference of some foreign species on the determination of alkannin under the optimized conditions. Some species commonly existing in biological samples were chosen for the interference study. The interference test was performed in the presence of 100-fold concentration of rutin, glucose, ascorbic acid, quercetin, dopamine, baicalin, acetaminophen, ethanol, $Cu^{2+}$, $Ca^{2+}$, $Zn^{2+}$, $Pb^{2+}$, $Mg^{2+}$, $Al^{3+}$, $Fe^{3+}$, $Br^{-}$, $NO_3^{-}$, and $SO_4^{2-}$ under the optimized conditions. The results suggested that they have no influence on the signals of 1.0 μmol $L^{-1}$ alkannin with deviation below 5.0 %.

In order to confirm the applicability of the proposed method, the sensor was used to detect alkannin in lithospermum samples by the standard addition method under optimized conditions. HPLC was introduced to confirm the results of these electrochemical tests. The HPLC data of alkannin is displayed in Table 1, which suggested that the peak areas of them had a good linear relationship with their concentrations. From the linearity of alkannin, the contents of the samples could be evaluated. These analyzes were performed in triplicate, and the results obtained are shown in Table 2. The results obtained by HPLC are in good agreement with the sensor determination (seen in Table 2, all the relative error are below 5 %), suggesting that this method is accurate. The recoveries are in the range of 98.5–106.3 %, and the relative standard deviations (RSDs) are all below 5 %. Additionally, the $F$ and Student $t$ tests were also studied, and the results are list in Table 2. It is stated that the $F$ and $t$ values obtained were all below the theoretical values ($F = 19.00$, $t = 4.30$), suggesting the highly accuracy and precision of the proposed sensor. Similarly, it is also revealed that the proposed method is a satisfactory and feasible method. Thus, the electrochemical sensor based on Au–PDDA-G can be efficiently used for sensitive determination of alkannin in natural samples.

## 4 Conclusion

In this study, a highly sensitive electrochemical sensor for the determination of alkannin in aqueous solution was fabricated based on the AuNPs–PDDA-G-modified GCE. The nanocomposite integrates the advantages of functionalized graphene and AuNPs, in which functionalized graphene with excellent conductivity and solubility provides a large specific surface area to increase the loading amount of alkannin, and the AuNPs provide an efficient interface and microenvironment for the electrochemical reaction of alkannin. Under the optimized conditions, the nanocomposite film-modified GCE was successfully employed for the voltammetric determination of alkannin with a low detection limit, wide linear range, and good selectivity. Finally, the proposed method was successfully applied to alkannin detection in the real drug samples with recovery ranging from 98.5 to 106.3 %.

**Acknowledgments** This study was supported by the National Natural Science Foundation of China (No. 20775030).

## References

1. Assimopoulou N, Karapanagiotis I, Vasiliou A, Kokkini S, Papageorgioul VP (2006) Biomed Chromatogr 20:1359
2. Papageorgiou VP (1980) Planta Med 38:193
3. Papageorgiou VP, Assimopoulou AN, Couladouros EA, Hepworth D, Nicolaou KC (1999) Angew Chem Int Ed 38:270

4. Spyros A, Assimopoulou AN, Papageorgiou VP (2005) Biomed Chromatogr 19:498
5. Zapp E, Brondani D, Vieira IC, Dupont J, Scheeren CW (2011) Electroanalysis 23:1124
6. Ochocka RJ, Rajzer D, Kowalski P, Lamparczyk H (1995) J Chromatogr A 709:197
7. Zhou L, Kang J, Fan L, Ma XC, Zhao HY, Han J, Wang BR, Guo DA (2008) J Pharm Biomed Anal 47:39
8. Li CH, Chen AJ, Chen XF, Chen XG, Hu ZD (2005) J Pharm Biomed Anal 39:125
9. Chen Z, Zhang LY, Chen G (2009) Electrophoresis 30:3419
10. Rogers KR, Becker JY, Wang J, Lu F (1999) Field Anal Chem Technol 3:161
11. Chaisuksant R, Voulgaropoulos A, Papageorgiou VP (1993) Analyst 118:179
12. Schedin F, Geim AK, Morozov SV, Hill EW, Blake P, Katsnelson MI, Novoselov KS (2007) Nat Mater 6:652
13. Tang LH, Wang Y, Li YM, Feng HB, Lu J, Li JH (2009) Adv Funct Mater 19:2782
14. Chen JL, Zheng XL, Miao FJ, Zheng JN, Cui XQ, Zheng WT (2012) J Appl Electrochem 42:875
15. Xu MR, Zhu HCh, Dong J, Ai ShY, Li R (2012) J Appl Electrochem 42:509
16. Niyogi S, Bekyarova E, Itkis ME, McWilliams JL, Hamon MA, Haddon RC (2006) J Am Chem Soc 24:7720
17. Liu KP, Zhang JJ, Yang GH, Wang CM, Zhu JJ (2010) Electrochem Commun 12:402
18. Xu ZA, Gao N, Dong SJ (2006) Talanta 68:753
19. Chen HJ, Wang YL, Wang YZh, Dong ShJ, Wang EK (2006) Polymer 47:763
20. Feng QL, Liu KP, Fu JJ, Zhang YZ, Zheng ZhX, Wang ChM, Du YL, Ye WCh (2012) Electrochim Acta 60:403
21. Hummers WS, Offeman RE (1958) J Am Chem Soc 80:1339
22. Zhang YZ, Gu YE, Lin ShX, Wei JP, Wang ZH, Wang ChM, Du YL, Ye WCh (2011) Electrochim Acta 56:8746
23. Chen JL, Yan XP (2010) J Mater Chem 20:4328
24. Zhou Y, Bao QL, Tang LA, Zhong YL, Loh KP (2009) Chem Mater 21:2950
25. Laviron E (1979) J Electroanal Chem 101:19
26. Du HJ, Ye JS, Zhang JQ, Huang XD, Yu CZ (2011) J Electroanal Chem 650:209
27. An J, Li JP, Chen WX, Yang ChX, Hu FD, Wang ChM (2013) Chem Res Chin Univ. doi:10.1007/s40242-013-2436-9